Network Architecture of Verticality Processing in the Human Thalamus

Julian Conrad, MD [1,2,3] Bernhard Baier, MD [4,5] Laurenz Eberle, MD,[1]
Ria Maxine Ruehl, MD,[1] Rainer Boegle, PhD,[1,3] Andreas Zwergal, MD,[1,3] and
Marianne Dieterich, MD[1,3,5,6]

Objective: Thalamic dysfunction in lesions or neurodegeneration may alter verticality perception and lead to postural imbalance and falls. The aim of the current study was to delineate the structural and functional connectivity network architecture of the vestibular representations in the thalamus by multimodal magnetic resonance imaging.

Methods: Seventy-four patients with acute unilateral isolated thalamic infarcts were studied prospectively with emphasis on the perception of verticality (tilts of the subjective visual vertical [SVV]). We used multivariate lesion–symptom mapping based on support-vector regression to determine the thalamic nuclei associated with ipsiversive and contraversive tilts of the SVV. The lesion maps were used to evaluate the white matter disconnection and whole brain functional connectivity in healthy subjects.

Results: Contraversive SVV tilts were associated with lesions of the ventral posterior lateral/medial, ventral lateral, medial pulvinar, and medial central/parafascicular nuclei. Clusters associated with ipsiversive tilts were located inferiorly (ventral posterior inferior nucleus) and laterally (ventral lateral, ventral posterior lateral, and reticular nucleus) to these areas. Distinct ascending vestibular brainstem pathways terminated in the subnuclei for ipsi- or contraversive verticality processing. The functional connectivity analysis showed specific patterns of cortical connections with the somatomotor network for lesions with contraversive tilts, and with the core multisensory vestibular representations (areas Ri, OP2-3, Ig, 3av, 2v) for lesions with ipsiversive tilts.

Interpretation: The functional specialization may allow both a stable representation of verticality for sensorimotor integration and flexible adaption to sudden changes in the environment. A targeted modulation of this circuitry could be a novel therapeutic strategy for higher level balance disorders of thalamocortical origin.

ANN NEUROL 2023;94:133–145

Verticality perception is essential for upright stance, bipedal locomotion, and spatial orientation in humans.[1–4] The estimation of verticality relative to the gravitational vector depends on otolith and semicircular canal inputs from the inner ear and is computed via an ascending neural network with the thalamus being a key hub.[5–8] Thalamic dysfunction may therefore critically affect verticality processing and thus cause postural imbalance and falls, as exemplified by thalamic astasia in focal ischemic lesions, thalamocortical pusher syndrome, or severe imbalance in patients with chronic deep brain stimulation (DBS) of the lateral thalamus (ventralis intermedius nucleus [Vim]).[9–12] Moreover, dysfunctions of thalamocortical structures also cause imbalance of body position with falls in neurodegenerative disorders such as supranuclear palsy[7,8]

Although at least 5 brainstem pathways for verticality processing are known (via the medial longitudinal fascicle [MLF], ascending Deiters tract [ATD], ipsilateral vestibulothalamic tract [IVTT], parapontine reticular formation [PPRF], and superior cerebellar peduncle [SCP]), there is some inconsistency about the functional and structural topography, as well as network circuitry at the thalamic level and above. Most authors conclude that graviceptive projections terminate in the lateral nuclear group of the thalamus and predominantly involve the main sensory nuclei (ventral posterior lateral [VPL] and ventral posterior medial [VPM]). Additional projections were observed to the ventral lateral nucleus (VL), the ventral posterior inferior nucleus (VPI), the parafascicular/centromedian nuclei (Pf/CM), the medial pulvinar (Pum), and the intralaminar nuclei. In two prior thalamic lesion studies, tilts of the subjective visual vertical (SVV), which can be considered a vestibular estimate of verticality, were associated with lesions of the lateral posterior nuclear group mirroring the homologous findings in nonhuman primates.[13,14] However, there is some debate about the direction-specificity of graviceptive inputs to thalamic subnuclei.[15] In a previous study, contraversive SVV tilts were associated with lesions of nuclei VL (ventro-oralis internus), Vim, VPL(ventralis caudalis), medialis–dorsalis, Pf/CM, and centralis lateralis, intralaminar, whereas ipsiversive tilts were located more inferiorly and medially, namely in the Pf and the nucleus endymalis (central medial ventral nucleus).[14]

The functional significance of the ipsiversive versus contraversive vestibulothalamic projections, as well as their cortical terminations, has not yet been delineated. Decoding of the organization principle behind thalamocortical graviceptive networks may be of general interest for the understanding of the physiology and pathology of higher level balance control. This may imply both acute and chronic vascular pathologies, as well as neurodegenerative disorders affecting thalamocortical circuits such as parkinsonian syndromes.

In this respect, the current study aimed to delineate the topography of thalamic nuclei that receive ipsiversive versus contraversive verticality signals and their up- and downstream connections using modern multivariate lesion symptom mapping (support-vector regression lesion symptom mapping [SVR-LSM]) and lesion–network mapping in a large cohort of patients with acute thalamic ischemia. Our hypotheses were: (1) a direction-specific processing of verticality exists across thalamic subnuclei with contraversive tilts located in the lateral group (VPL/VPM, VL [Vim]) and ipsiversive tilts in the VPI and inferior parts of VPL/VPM; (2) upstream

vestibular pathways from the brainstem target different thalamic subnuclei following this basic principle of graviceptive processing (contraversive: MLF, ATD, PPRF; ipsiversive: IVTT/medial lemniscus [ML], SCP); and (3) the distinct topographical and hodological organization of verticality processing is paralleled by functionally specialized projections to cortical networks, namely to somatomotor networks for thalamic subnuclei with contraversive graviceptive tuning and inferior insular cortex, parietal operculum, and adjacent (retro)-insular cortex for subnuclei with ipsiversive sensory (graviceptive) properties. In summary, we postulate that graviceptive signals are distributed to functionally specialized cortical networks via specific thalamic subnuclei to allow for both a stable perceptive representation of verticality and a flexible integration of graviceptive information in sensorimotor and postural adaptation.

Patients and Methods

Patient Selection and Clinical Evaluation

We prospectively studied 74 patients who presented to the University Hospitals of the University of Munich or University of Mainz between 2004 and 2022. Inclusion criteria were as follows: evidence of an acute unilateral circumscribed ischemic thalamic infarct (n = 73) or hemorrhage (n = 1), confirmed by magnetic resonance imaging (MRI), and the ability to complete the measurement of the SVV. Exclusion criteria were: absence of an ischemic lesion on diffusion MRI, bilateral or multifocal infarcts, prior stroke, tumor, vascular malformation, edema (ie, compression of cerebrospinal fluid [CSF] space, shift of midline structures), severe white matter hyperintensities (WMH; Fazekas grade > 1 for periventricular WMH and deep WMH), and cognitive impairment or impaired vigilance so that patients were unable to complete the neurological and neuro-otological examination.

All patients received a neurological and a dedicated neuro-orthoptic examination, which included the measurement of the SVV. A mean of >2.5° of the 8 measurements of the static SVV determined binocularly was considered a pathologic roll-tilt of static SVV.[16] Measurements were carried out in complete darkness using a hemispheric dome with a randomized dot pattern to eliminate visual cues for orientation. Spontaneous nystagmus, subjective vertigo/dizziness, somatosensory deficits, dysarthria, and ataxia were classified as present or not.

The current sample of 74 patients included 33 patients from a prior lesion study[14] and 13 patients from a longitudinal study on vestibular thalamic

compensation; 28 patients were recruited at the University Hospital in Munich between 2013 and 2022.[14,17]

Imaging and Lesion Segmentation

Ischemic infarcts were delineated on acute phase diffusion-weighted imaging (DWI) sequences (3mm, echo time [TE] = 880 milliseconds, repetition time [TR] = 1400 milliseconds, 48 slices) using MRIcron (https://www.nitrc.org/projects/mricron). All lesion maps were normalized to $1 \times 1 \times 1mm^3$ MNI152 space using the *Clinical Toolbox* implemented in SPM.[18] The lesion maps were evaluated by two experienced raters for congruency (J.C., L.E., or B.B.) using anatomical neighboring relationships (basal ganglia, internal capsule, third ventricle, anterior/posterior commissure, rostral midbrain [red nucleus]) with information from the acute phase DWI and fluid-attenuated inversion recovery sequences. If discrepancies between raters were observed (n = 17), the corrected lesion was evaluated again by both raters until an agreement was reached. To adjust the lesion header information for the usage in the BCB toolbox (http://toolkit.bcblab.com), we applied an in-house script based on the ImCalc function in SPM. The data of 14 cases was discarded because no dedicated neuro-otological testing (n = 11) or MRI had been carried out (n = 3; all not part of the analyses).

Support-Vector Regression Lesion Symptom Mapping

Multivariate SVR-LSM was used to detect relevant associations of damaged voxels with the degree of tilt of the SVV.[19,20] In contrast to the mass-univariate approach, SVR-LSM takes the neighboring relationships of affected voxels into account. This is particularly important because a statistical independence of the affected voxels cannot be assumed given the nonrandom distribution of brain lesions.[20] For the SVR, the lesion maps were vectorized, and lesion volume was regressed out of the lesion and behavioral data. Hyperparameters were kept in the default setting of the SVR-LSM toolbox.[20] First, all lesions were included in the SVR-LSM model using the degree of tilt as the behavioral variable. For the differential analysis of contraversive versus ipsiversive tilts of the SVV, lesions were flipped to the right. Lesion threshold was set to 10% of the total sample.[21] To control for type II errors, extensive permutation testing (10,000 permutations) and correction for multiple comparisons using the false discovery rate (FDR) function in FSL (http://fsl.fmrib.ox.ac.uk/fsl/fslwiki/FDR) were applied. All results are depicted with the respective FDR-corrected significance thresholds. The resulting statistical maps (in MNI152 space) for the tilt effects were transformed into binary masks that were used in the disconnectome and lesion–network mapping analyses.

Disconnectome Mapping

The tractography-based method implemented in the BCB toolkit (http://toolkit.bcblab.com/) was used to calculate the probability of disconnection of specific white matter tracts for each lesion.[22,23] High-resolution (7T) tractography data of 170 healthy participants from the Human Connectome Project (HCP) were used to track fibers that pass through each individual lesion based on a parcellation by Rojkova et al.[24] The attribution of fibers to a specific target is based on anatomical expertise of the toolbox developers.[25] The patients' lesions in MNI152 space were registered to the native space of each healthy participant's tractography data using affine and diffeomorphic deformations.[26,27] This seed was then used to perform the tractography in TrackVis (http://www.trackvis.org/). The results were transformed to visitation maps, binarized, and registered to MNI152 space. From these maps, the percentage of overlap of each voxel in the normalized subject visitation maps was depicted as the voxelwise probability of disconnection for each lesion. The number of voxels within the individual disconnectome map was thresholded at 0.5 (50% or higher probability of disconnection).

SVR–Disconnectome Mapping

Constructed disconnectome maps were binarized and then fed into an SVR-LSM analysis using the same parameters as described above for the SVR-LSM analysis. The lesion size has influence on the number of streamlines passing through the lesion and thus on the resulting voxelwise disconnectome maps. For the analysis of the binarized lesion-disconnection maps, the volume of the disconnectome maps was regressed out of the lesion and the behavioral data. This approach was described earlier.[21] As small brainstem tracts such as the vestibulothalamic projections are not integrated as separate entities in the toolbox, the attribution of the disconnectome SVR-LSM is based on expert evaluation of the brainstem anatomy.

Lesion–Network Mapping

The 100 Unrelated Subjects preprocessed resting-state functional MRI (fMRI) dataset from the HCP (https://www.humanconnectome.org/; release Q3) was used for this analysis. These data contained fMRI resting-state acquisitions from 100 unrelated subjects (54 females, 46 males, mean age = 29.1 ± 3.7 years).

The resting-state fMRI data were acquired as part of the HCP 900 data release using a gradient-echo echo planar imaging sequence (TR = 720 milliseconds, TE = 33.1 milliseconds, flip angle = 52°, field of view = 208 × 180, matrix size = 104 × 90, $2mm^3$ isotropic, 72 slices, multiband factor = 8, echo spacing = 0.58 milliseconds, band width = 2290 Hz/pixel, 2 sessions,

1200 volumes). Axial oblique acquisitions alternated between phase encoding in a right-to-left and left-to-right direction.[28] Data were processed following the HCP functional preprocessing guidelines.[29,30] Briefly, processing steps included artifact removal, motion correction, and registration to standard Montreal Neurological Institute space in volumetric format (MNI152 space).[30] The functional connectivity analysis was performed using CONN toolbox version 20b (http://www.nitrc.org/projects/conn) for MATLAB (version 2019b).[31] For denoising, the following time series were used as covariates in a nuisance regression model; white matter and CSF confounds were each considered with their first 5 principal components. Furthermore, 6 principal temporal components of the movement parameters (3 translation and 3 rotation parameters) were used. Images were denoised with a temporal band-pass filter (0.008–0.09Hz).

All results are depicted on a high-resolution 7T template using *MRIcroGL* (https://www.nitrc.org/projects/mricrogl).[32] Surface renderings were generated using *Surf Ice*. (https://www.nitrc.org/projects/surfice/) Ring connectomes were generated using the results from the SVR-LSM analysis, transformed into masks in MNI152 space and atlas regions of interest implemented in the CONN toolbox.

Patient Consent and Data Availability
The study was performed in accordance with the 1964 Declaration of Helsinki and approved by the institutional review board of Ludwig Maximilian University of Munich, Germany, and the University of Mainz, Germany. All patients gave informed written consent to participate in the study. The lesion maps from the Munich cohort will be publicly available (https://osf.io/4shmb/) upon publication. The Mainz dataset is not publicly available due to lack of consent for data sharing by the patients.

Results
Clinical Characteristics
An overview of the clinical and demographic data for patients with lesions associated with ipsiversive and contraversive tilts of the SVV is given in the Table . A lesion overlap of all lesions (flipped to the right) is shown in Figure 1A. Lesion volumes were not significantly different between right- and left-sided lesions (Mann–Whitney U test, $p = 0.786$) as well as between ipsiversive and contraversive SVV tilts (Mann–Whitney U test, $p = 0.695$). Lesions were predominantly located paramedian or posterolateral (territories of the paramedian and thalamogeniculate arteries, respectively). Right- and left-sided lesions were equally common in the group with ipsiversive tilts

TABLE. Clinical and Demographic Data of the Patients with Acute Unilateral Thalamic Strokes with Ipsiversive and Contraversive Tilts of the SVV

	Ipsiversive Tilt, n= 33		Contraversive Tilt, n= 41	
Demographic data				
Age, median yr (range, IQR)	74.0 (39–86, 16)[a]		72.0 (38–90, 27)	
Gender n (%)				
Female	18 (54.5)		19 (46.3)	
Male	15 (45.5)		22 (53.7)	
Clinical data				
Infarct side n (%)				
Right	17 (51.5)		17 (41.5)	
Left	16 (48.5)		24 (58.5)	
Lesion volume, median ml (range, IQR)	0.56 (0.01–4.52, 1.36)[b]		0.55 (0.06–5.26, 0.98)	
SVV, median degrees (range, IQR)	3.2 (0–11.5, 4.15)[c]		2.8 (0–21.5, 5.8)	

Symptoms	n	%	n	%
Spontaneous nystagmus[d]	2/33	6.1	1/41	2.4
Vertigo[d]	3/33	15.2	12/41	29.3
Skew deviation[d]	11/33	24.2	12/41	29.3
Double vision[d]	11/33	33.3	10/41	24.4
Contralateral paresis	18/33	54.6	25/41	61.0
Ataxia	13/33	39.4	13/41	31.7
Contralateral somatosensory deficit	15/33	45.6	22/41	53.7
Dysarthria	12/33	36.4	9/41	22.0
Spatial neglect	2/33	6.1	1/41	2.4
Visual field defect	1/33	3.0	1/41	2.4

Abbreviations: IQR = interquartile range; SVV = subjective visual vertical.
[a]Kolmogorov–Smirnoff = 0.178, $p < 0.001$; Mann–Whitney U = 190.5, $p = 0.478$; n = 74.
[b]Kolmogorov–Smirnoff = 0.215, $p < 0.001$; Mann–Whitney U = 712.5, $p = 0.695$; n = 74.
[c]Kolmogorov–Smirnoff = 0.148, $p = 0.002$; Mann–Whitney U = 674, $p = 0.987$; n = 74.
[d]Indicates involvement of the rostral midbrain in paramedian infarcts.

(17 left-sided lesions, 16 right-sided lesions). There was a preponderance of left-sided lesions in the patients with contraversive tilts of the SVV (left-sided lesions, n = 24; right-sided lesions, n = 17; χ^2 test, $p = 0.546$). The mean degree of SVV tilt was not significantly different between ipsiversive and contraversive tilts ($p = 0.987$, Mann–Whitney U test). Other vestibular (rotatory vertigo, nystagmus, skew deviation) deficits occurred in

fewer than one third of each group. The same was true for higher order spatial deficits (neglect) or visual field deficits. Apart from SVV tilts, contralateral paresis and somatosensory deficits were the most common deficits reported. Additional involvement of the eye–head coordination centers in the rostral midbrain (interstitial nucleus of Cajal) was evident in patients who presented with skew deviation and/or rotational
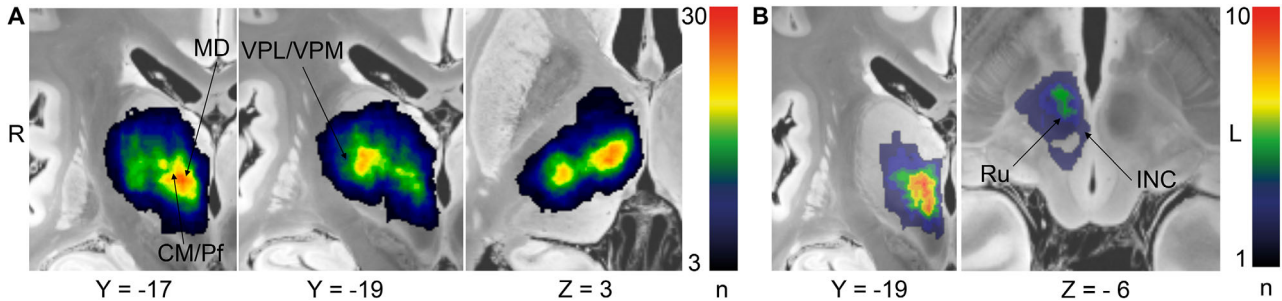

FIGURE 1: (A) Lesion distribution of all thalamic lesions. All lesions were flipped to the right. Lesions were centered around the lateral nuclear group (ventral lateral nucleus, ventral posterior lateral nucleus [VPL]) and the paramedian thalamus (mediodorsal nucleus [MD], central medial/parafascicular nucleus complex [CM/Pf]). Warmer colors indicate a higher number of overlapping lesions. (B) Paramedian infarcts of the thalamus also affected the rostral midbrain. INC = interstitial nucleus of Cajal; L = left; R = right; Ru = red nucleus; VPM = ventral posterior medial nucleus.
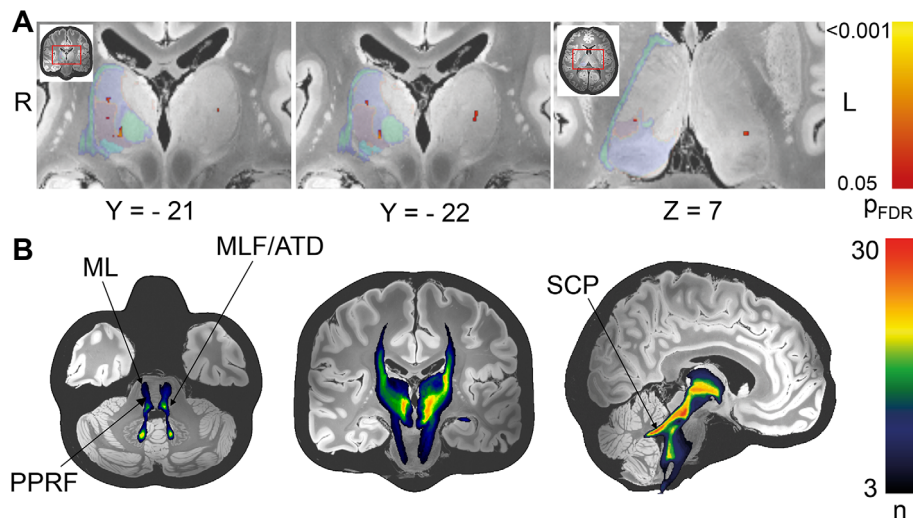

FIGURE 2: (A) Support-vector regression lesion symptom mapping analysis of all thalamic lesions (combined analysis of left- and right-sided thalamic lesions, n = 74). Clusters associated with tilts of the subjective visual vertical were located bilaterally. In the left hemisphere, only one cluster in the ventral posterior lateral (VPL)/ventral posterior medial (VPM) nucleus was detected. In the right hemisphere, a similar cluster was found in VPL/VPM. Additional clusters were located in the paramedian group (border zone of VPL/VPM with the central medial/parafascicular nucleus complex [CM/Pf]) and in the medial pulvinar. Clusters are depicted with the respective false discovery rate-corrected significance thresholds ($p_{FDR} < 0.05$) after extensive permutation testing (10,000 permutations). Thalamic nuclei are underlaid with different colors to depict nuclei borders[53]: white = ventral lateral nucleus; red = medial pulvinar; violet = VPL/VPM; cyan = ventral posterior inferior nucleus; green = CM/Pf, reticular nucleus. (B) Overlap of disconnectome maps of left- and right-sided lesions. The white matter projections passing through the thalamic lesions connected the thalamus with the pontomedullary brainstem and the cerebellum (deep cerebellar nuclei and vestibulocerebellar lobule IX). These were located in the region of the medial longitudinal fascicle (MLF) and ascending tract of Deiters (ATD), which cannot be distinguished from the MLF due to its close proximity to the former structure. Additional white matter projections were located in the medial lemniscus (ML) and the parapontine reticular formation (PPRF). The number of overlapping lesion-associated disconnectome maps on the left and right side are shown. Warmer colors represent a higher degree of overlap of the disconnectome maps. All maps were created using the default setting of a probability of 0.5 or higher of disconnection in a tractography dataset of 170 healthy individuals for each lesion seed. L = left; R = right; SCP = superior cerebellar peduncle.
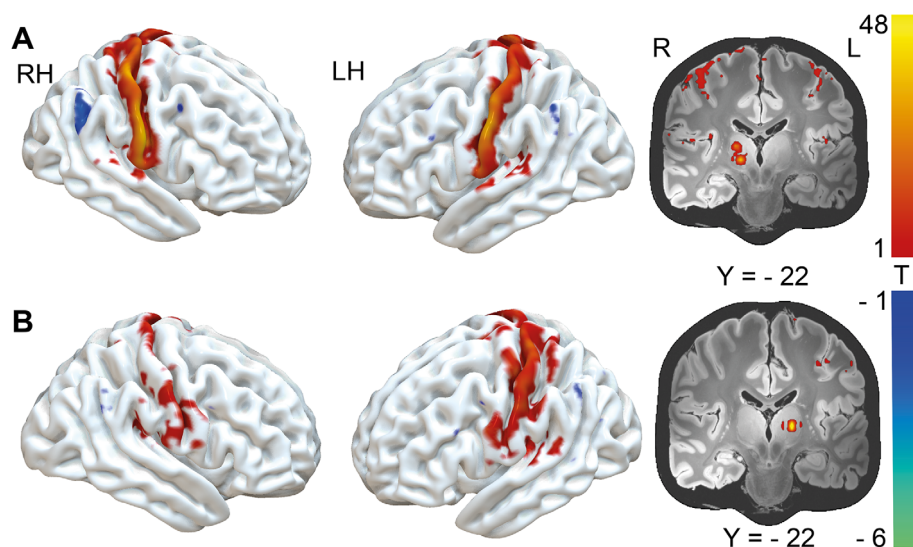
FIGURE 3: Lesion–network mapping of left- and right-sided lesions associated with tilts of the subjective visual vertical. For this analysis, the results from the support-vector regression lesion symptom mapping analysis were binarized and used as seed for a whole brain functional connectivity (fc) analysis. (A) The right-sided thalamic lesion seed showed fc with the somatosensory cortex including the parieto-opercular (retro-)insular cortex in both hemispheres. (B) Lesion–network mapping of the left-sided thalamic lesion seed showed fc with the somatosensory cortex. Negative correlations were found with the supramarginal gyrus and ventrolateral prefrontal cortex for both lesion seeds. The fc results are depicted with their peak t score intensity after nonparametric permutation testing (threshold-free cluster enhancement); $p_{FDR} < 0.05$ on the cluster level. L = left; FDR = false discovery rate; LH = left hemisphere; R = right; RH = right hemisphere.
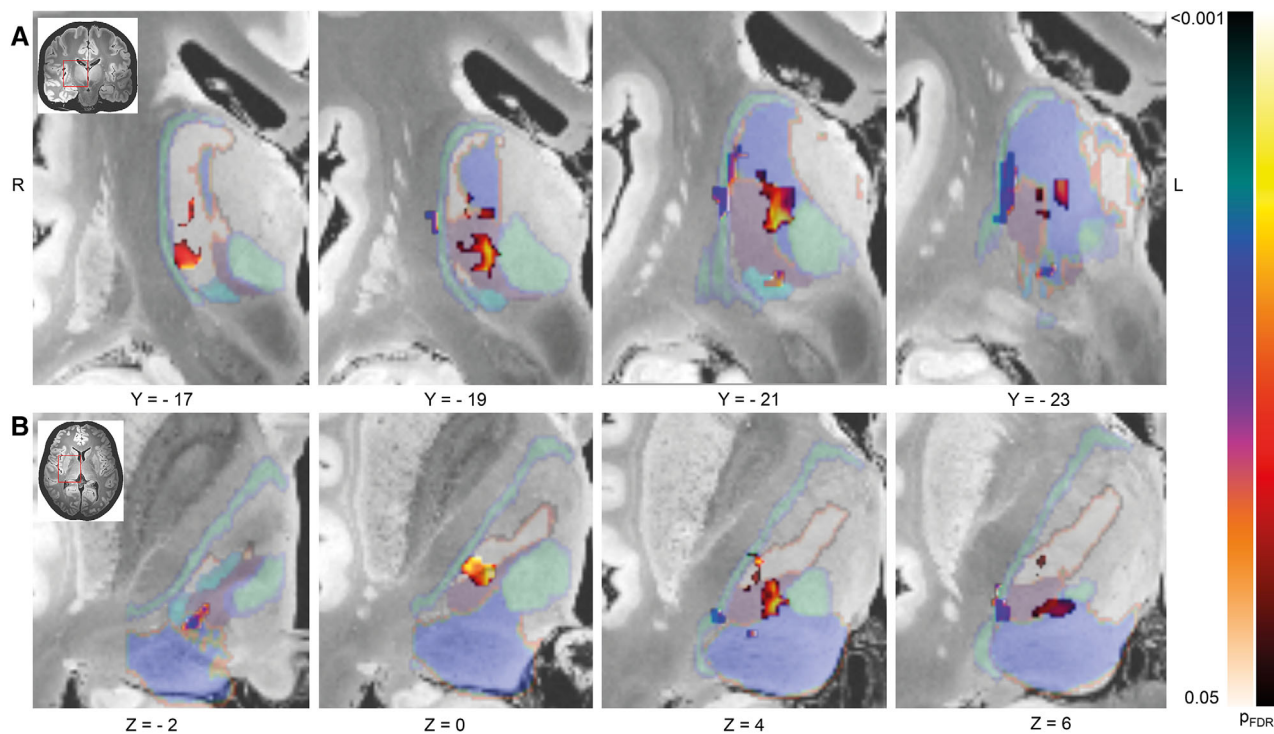
FIGURE 4: (A) Coronal slices and (B) axial slices of support-vector regression lesion symptom mapping (SVR-LSM) for lesions that caused contraversive tilts (hot color scheme). Significant clusters were found in the lateral nuclear group (ventral lateral nucleus [VL], ventral posterior lateral [VPL]/ventral posterior medial [VPM]) and the paramedian group (medial pulvinar, central medial/parafascicular nucleus complex [CM/Pf]). Orange–green color scheme: SVR-LSM for lesions that caused ipsiversive tilts. The main affected nuclei were the ventral posterior inferior nucleus (VPI) bordering VPL/VPM and the reticular nucleus (Rt) at the border of the lateral VL/VPL. The lesions causing ipsiversive tilts were located more laterally and inferiorly to the lesions that caused contraversive tilts. Clusters are depicted with the respective false discovery rate (FDR)-corrected significance thresholds ($p_{FDR} < 0.05$) after extensive permutation testing (10,000 permutations). Thalamic nuclei are underlaid with different colors to depict nuclei borders[53]: white = ventral lateral nucleus; red = medial pulvinar; violet = VPL/VPM; cyan = VPI; green = CM/Pf, Rt.
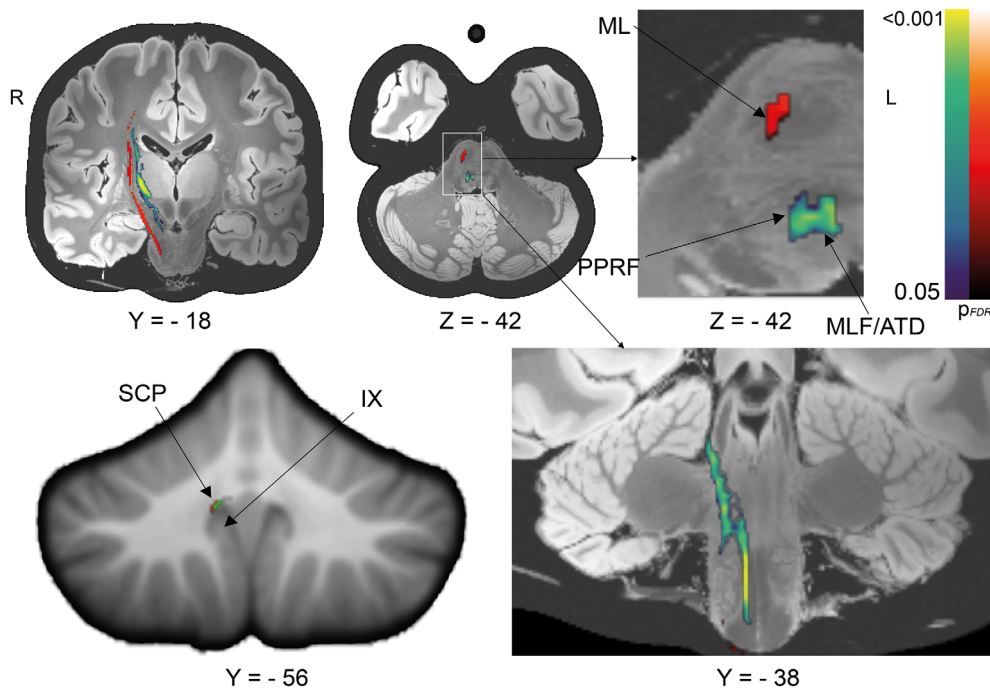
FIGURE 5: White matter connections associated with contraversive (yellow/green) and ipsiversive tilts (red). The white matter projections associated with contraversive tilts of the subjective visual vertical (yellow/green) were found in close proximity to known vestibulothalamic projections in the medial longitudinal fascicle (MLF)/ascending Deiters tract (ATD) and the parapontine reticular formation (PPRF) as well as to the cerebellum via the superior cerebellar peduncle (SCP). They seem to terminate around the deep cerebellar nuclei and vestibulocerebellar lobule IX. The cortical projections seem to reach mainly the somatosensory and motor cortex. White matter projections associated with ipsiversive tilts (red) were observed in the medial lemniscus (ML; ipsilateral vestibulothalamic tract) and the SCP. These projected more laterally to the thalamus and also terminated in the somatosensory and motor cortex. Clusters are depicted with the respective false discovery rate (FDR)-corrected significance thresholds ($p_{FDR} < 0.05$) after extensive permutation testing (10,000 permutations). L = left; R = right.
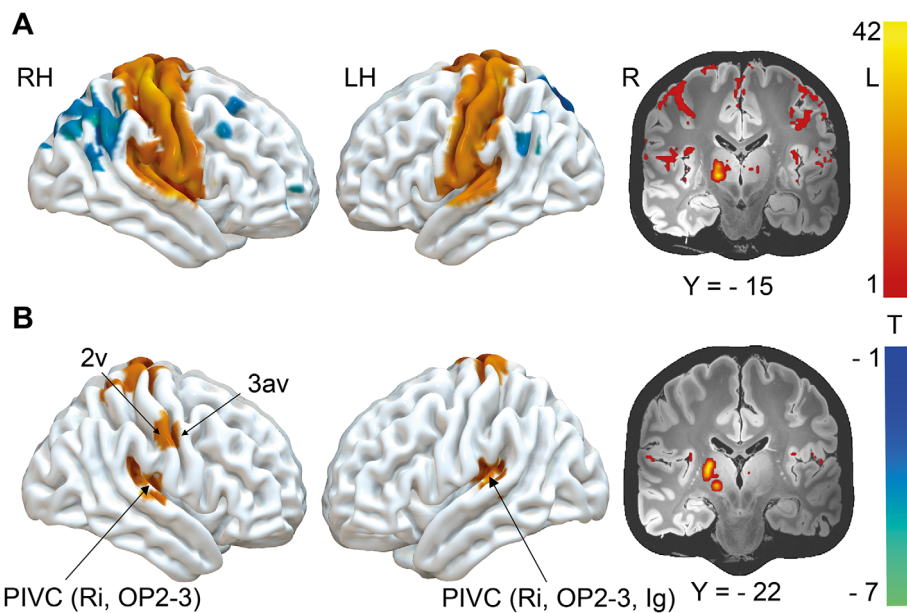
FIGURE 6: Lesion–network mapping using the results from the support-vector regression lesion symptom mapping as seeds for whole brain functional connectivity (fc). (A) The lesion–functional connectivity network (FCN) associated with contraversive tilts included the somatosensory and motor cortex and extended to the core vestibular cortical areas in the parieto-opercular (retro-) insular vestibular cortex (PIVC) and S2 (warm color scheme). Negative correlations were found with the inferior parietal lobule - IPL (areas PG, PF); blue–green color scheme. (B) The lesion-FCN associated with ipsiversive tilts was restricted to the core cortical vestibular hubs in PIVC (areas area retroinsularis [Ri], parietal opercular [OP] 2-3 in the right hemisphere [RH] and Ri, OP2-3, insular granular cortex [Ig] in the left hemisphere [LH]), and 3av and 2v. The fc results are depicted with their peak t score intensity after nonparametric permutation testing (threshold-free cluster enhancement); $p < 0.05$ false discovery rate-corrected on the cluster level. L = left; R = right.

vertigo due to the common vascular supply of the paramedian thalamus and the paramedian rostral midbrain (see Fig 1B).[33]

Left and Right Thalamic Infarcts

Support-Vector Regression Lesion Symptom Mapping
Using SVR-LSM, left- and right-hemispheric clusters that were associated with absolute tilt of the SVV were detected. The cluster in the left thalamus was located in the VPL/VPM nucleus (centroid: $x = -16$, $y = -22$, $z = 6$, cluster volume $= 0.02mm^3$). Right thalamic clusters were also found in VPL/VPM. Additionally, small scattered clusters were found at the border of VPL/VPM and Pf/CM and in the Pum (medial cluster centroid: $x = 8$, $y = -19$, $z = 5$, volume $< 0.01mm^3$ [10 voxels]; ventral cluster centroid: $x = 14$, $y = -21$, $z = 2$, volume $= 0.03mm^3$; lateral cluster centroid: $x = 16$, $y = -18$, $z = 5$, volume $= 0.01mm^3$; Fig 2A).

Disconnectome Maps. The disconnectome maps (fibers passing through each lesion with a probability > 0.5) are depicted in Figure 2B. The fibers of left- and right-sided infarcts connect the thalamus with the pontomedullary brainstem via the MLF/ATD, the ML, and the PPRF. The affected thalamic nuclei were also structurally connected with the deep cerebellar nuclei and vestibulocerebellar lobule IX via the SCP.

Lesion–Network Mapping. The results from the SVR-LSM were used as the seeds for a whole brain functional connectivity (fc) analysis. Here, the right thalamic seeds were functionally connected with the somatosensory cortex bilaterally and also reached the parieto-opercular (retro-) insular vestibular cortex (PIVC). Anticorrelations were found with the supramarginal gyrus and the ventrolateral prefrontal cortex for both lesion seeds (Fig 3).

Lesions with Ipsiversive versus Contraversive Tilts of the SVV

Support-Vector Regression Lesion Symptom Mapping. The absolute values of SVV tilt were used for the analysis (ie, a tilt of $-3.1°$ was scored as $3.1°$). Patients with ipsiversive and contraversive tilts were considered separately. Clusters associated with contraversive tilt of the SVV were located in the VPL, VL, Pf/CM, and medial pulvinar nuclei (rostral dorsal cluster centroid: $x = 17$, $y = -17$, $z = 6$, volume $= 0.03mm^3$; ventral caudal cluster centroid: $x = 16$, $y = -20$, $z = 4$, volume $= 0.13mm^3$; Fig 4). In contrast, lesions associated with ipsiversive tilt were located inferiorly and more laterally in VPI and inferior VPL/VPM
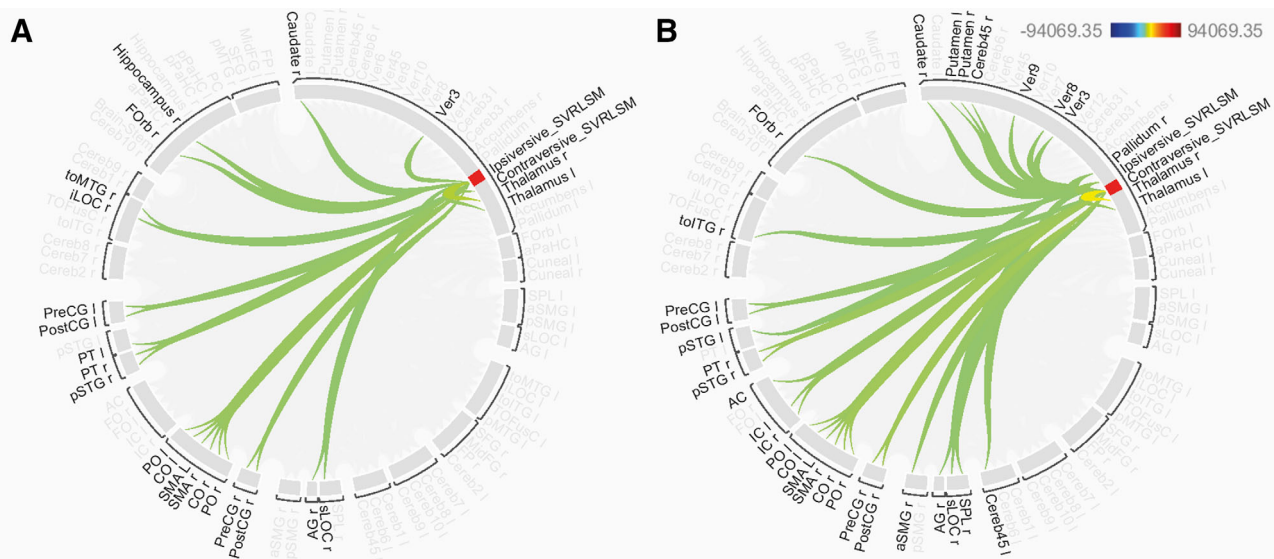
FIGURE 7: (A) Ring connectome of the seed associated with ipsiversive tilts; fc was found with the PO, CO, PreCG, PostCG, SMA bilaterally, and vermal lobule 3 (Ver3). Additional unilateral fc was found with the temporo-occipital parts of the right middle temporal gyrus (toMTG), inferior parts of the right lateral occipital cortex (iLOC), pSTG, temporal pole (PT), angular gyrus (AG), hippocampus, caudate nucleus, and FOrb. (B) Ring connectome of the seed associated with contraversive tilts: functional connectivity (fc) was found with the insula (IC), parietal operculum (PO), central operculum (CO), supplementary motor areas (SMA), pre- and postcentral gyrus (PreCG, PostCG), posterior superior temporal gyrus (pSTG), putamen, and cerebellar lobules 4 and 5 (Cereb45) bilaterally. Additional fc was found with the right superior parietal lobule (SPL), angular gyrus (AG), anterior supramarginal gyrus (aSMG), superior lateral occipital cortex (sLOC), temporo-occipital part of the inferior temporal gyrus (toITG), frontal orbital cortex (FOrb), caudate, pallidum, and nucleus accumbens (AC). l = left-sided areas; r = right-sided areas. Color intensity and line thickness represent the degree of correlation between the seed region and the respective cortical areas. All results are presented after extensive nonparametric permutation testing and correction for multiple comparisons using false-discovery correction (familywise error), thresholded at *p* < 0.05 on the cluster level. SVRLSM = support-vector regression lesion symptom mapping.

and in a small cluster in the Pum (centroid of the VPI cluster: x = 16, y = −22, z = −3, volume = 0.01mm^3). A further cluster was located in the lateral VPL/VL and the adjacent reticular nucleus (centroid of the lateral VPL cluster: x = 22, y = −23, z = 8, volume = 0.04mm^3; see Fig 4). There was no overlap between clusters associated with ipsiversive and contraversive tilts.

SVR–Disconnectome Symptom Mapping. White matter connections associated with contraversive tilts of the SVV were detected in the brainstem tegmentum in 2 separate clusters likely reflecting the MLF, ATD (in close proximity to the MLF), and PPRF. Additional streamlines were found in the SCP. The streamlines entered the inferior lateral thalamus around VPI and VPL/VPM and proceeded dorsally and laterally through VL to the primary somatosensory and motor cortex. Additional streamlines passed anteriorly to the prefrontal cortex (Fig 5).

White matter connections that were associated with ipsiversive SVV tilt were distinct from those associated with contraversive tilt. White matter connections traveled with the ML (corresponding to previously described IVTT) and in part bypassed the thalamus more laterally adjacent to the thalamic cluster associated with ipsiversive tilt from the SVR-LSM analysis and proceeded toward the primary somatosensory and motor cortices (see Fig 5).

Lesion–Network Mapping. The results from the SVR-LSM analysis were used as seeds to compute the whole brain fc of the clusters of the thalamic regions associated with ipsiversive and contraversive tilts of the SVV. Here, the fc network of the thalamic clusters associated with contraversive tilts connected the thalamus with the somatomotor network, spanning the entire primary sensory and motor cortices and extending into the PIVC (parietal operculum, granular, area Ri, granular insular cortex). A negative correlation was found mainly with the inferior parietal lobule (areas PG, PF; Fig 6A).

In contrast, the fc network of the lesion seed for ipsiversive tilt was far more restricted to the primary multisensory vestibular cortical areas of the PIVC (areas Ri, OP2-3, 4), area 3av, and area 2v (see Fig 6B).

A ring connectome of the lesion seeds for ipsiversive and contraversive tilts of the SVV depicts the differential connectivity with other areas of the cerebral cortex and subcortex (Fig 7).

Discussion

The main findings of this study in 74 patients with acute unilateral thalamic strokes causing side-specific tilts of verticality perception were as follows. (1) Distinct thalamic subnuclei were associated with either ipsiversive or contraversive SVV tilts. This topography replicates findings from tracer studies in nonhuman primates. Contraversive tilts were associated with lesions of the medial VPM/VPL, the Pum, the VL, and the Pf/CM complex. Lesions associated with ipsiversive tilts were located inferiorly and laterally to the latter in the border zone of VPI and VPM/VPL and in the lateral VPL adjacent to the reticular nucleus (Rt). (2) The disconnectome-based lesion–symptom mapping approach demonstrated 2 distinct sets of white matter projections associated with SVV tilts. Contraversive tilts were associated with structural disconnection of the MLF/ATD and PPRF. Ipsiversive tilts were associated with white matter projections that proceeded along the ML via IVTT to the inferior lateral thalamus (VPI, lateral VPL, and Rt). White matter projections for both ipsiversive and contraversive tilts were detected in the SCP. (3) Using lesion–network mapping, unique network properties of the thalamic areas associated with ipsiversive and contraversive tilts of the SVV were demonstrated. The contraversive graviceptive network projected to the entire somatomotor network, which included the multisensory vestibular core areas PIVC and area 3av. The ipsiversive graviceptive network almost exclusively projected to the vestibular cortical key structures (PIVC, 3av, 2v).

Taken together, we present a comprehensive network architecture of verticality processing in the thalamus that connects the brainstem and cerebellum with the primary multisensory vestibular, somatosensory, and motor cortex areas (Fig 8). The findings provide the basis for the evaluation of the pathophysiological relevance of verticality processing for higher level disorders of postural control during stance and gait (such as strategic vascular lesions or neurodegenerative disorders affecting thalamocortical networks). Furthermore, thalamic topography and hodology of verticality processing may be important for the placement and tuning of DBS electrodes in thalamic subnuclei (eg, for tremor) to avoid detrimental long-term effects for balance control.

Thalamic Nuclei Associated with Verticality Perception

An association of contraversive SVV tilts with lesions of the VPL/VPM, VL, Pum, and Pf/CM nuclei was found, whereas ipsiversive tilts were associated with more lateral and inferior lesions that included the border zone of VPL/VPM and VPI, as well as the lateral VPL/VL and Rt. This is in line with prior work, which described a similar distribution of affected thalamic nuclei.[14,34] A dissociation of thalamic nuclei involved in ipsiversive versus contraversive SVV tilts has been demonstrated before in a univariate voxelwise lesion–behavior mapping MRI
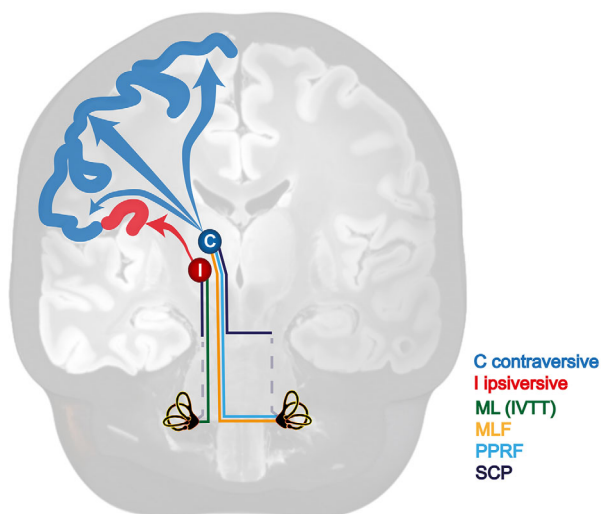
FIGURE 8: Schematic depiction of the vestibulothalamocortical network associated with ipsiversive (I; red) and contraversive (C; blue) tilts of the subjective visual vertical. Vestibulothalamic brainstem pathways reach the ventral posterior inferior nucleus and lateral ventral posterior lateral/reticular nucleus mostly via the ipsilateral vestibulothalamic tract (IVTT)/medial lemniscus (ML) and superior cerebellar peduncle (SCP). Lesions to these pathways lead to ipsiversive tilts. Functional connections with the cortex are located in the parietoinsular vestibular cortex (red). Further vestibulothalamic brainstem pathways reach mainly the lateral nuclear complex via the medial longitudinal fascicle (MLF)/ascending Deiters tract, parapontine reticular formation (PPRF), and superior cerebellar peduncle (SCP). These nuclei are functionally connected with the entire somatomotor network (blue).

study.[14] The current study refined the topographical organization of verticality processing in the thalamus based on a higher number of patients and a state-of-the-art multivariate SVR-LSM approach. The thalamic subnuclei associated with SVV tilts in the current study closely match the results from tracer studies in nonhuman primates, which found vestibulothalamic projections mainly in VPL, VL, Pum, and VPI.[5,35,36] Additionally, thalamocortical projections from or to the multisensory vestibular core areas (PIVC, area 3av) were described in the VPL/VPM, VL, VPI, and Rt in a similarly scattered distribution.[6]

Upstream Graviceptive Pathways Connecting the Vestibular Nuclei and Cerebellum with the Thalamus

In nonhuman primates, five ascending tracts have been described that convey vestibular signals: the MLF, the ATD, the SCP, the IVTT adjacent to the ML, and fiber tracts from the PPRF.[5,34,37–42] Human studies in stroke patients with associated SVV tilts reinforced the relevance of the MLF, the SCP, and the IVTT close to the ML for graviceptive processing.[42–45] Importantly, lesions of the MLF/ATD/PPRF tracts mostly resulted in contraversive

tilts of the SVV, whereas lesions of the IVTT/ML pathway induced ipsiversive tilts.[42,44,45] Lesions of the SCP projections may cause contra- or ipsiversive SVV tilts.[43,46] Anatomically, both the IVTT/ML and SCP course through the VPI.[47] Using disconnectome mapping and disconnectome-based SVR-LSM, we now found evidence for white matter projections connecting the pontomedullary brainstem and cerebellum via the thalamic nuclei with the somatosensory and motor cortex. These connections closely match the location of the MLF and ATD for contralateral projections, the IVTT/ML for ipsilateral projections, and the SCP for bidirectional information.

Thalamocortical Projections for Verticality Processing

The *structural* disconnectome–LSM approach yielded thalamocortical connections of the thalamic lateral nuclear group with the primary sensory and motor cortices. The main cortical projection zones of these nuclei (namely, VPL, VL) are the somatosensory and motor cortex.[47] In addition, we expected to find thalamocortical disconnection with the PIVC, which was not the case in the current data, likely due to methodological limitations. In the tractography approach, streamlines follow the dominant fiber direction of the white matter tract, which undisputedly runs to the primary motor and primary sensory cortex areas if seeded in the VPL/VL. Thus, smaller white matter connections with secondary somatosensory cortex or PIVC might have been overlooked. Furthermore, the claustrum acts as a natural obstacle between the thalamus and the insular cortex, making detection of such tracts even more difficult. Previous studies have shown that if a seed is directly placed in the PIVC, projections to the lateral nuclei of the thalamus can be identified in healthy subjects, as well as in patients with cortical insular–opercular infarcts.[23,48]

It is noteworthy that we detected thalamocortical *functional* connectivity with the multisensory vestibular core network including the PIVC in the lesion–network mapping (fc) analysis. We disclosed distinct thalamocortical projections for the lesion seeds associated with contraversive and ipsiversive tilts. The ipsiversive tilt seed projected to the vestibular network areas PIVC (area Ri, OP2-3, Ig), 3av, and 2v almost exclusively, whereas the contraversive tilt seed projected to the entire somatomotor network. In line with the ipsiversive tilt network, tracer studies in nonhuman primates have established connections of the PIVC (Ri, granular insular cortex) with the VPI and ventral posterior oralis; the latter corresponds to the lateral VPL in the nomenclature of the present study).[6] The finding of a direction-specific thalamocortical network engaged in

verticality processing is novel and follows the existing literature on functional lateralization of brain networks.[49]

What Is the Need for Distinct Thalamocortical Networks for Verticality Processing?

Graviceptive vestibular signals are essentially involved in various key domains of human behavior such as motor control of head and body position during stance and locomotion, perception of body motion and position, and orientation and navigation in 3-dimensional (3D) space. Given these variable demands, it is conceivable that graviceptive signals are processed in parallel upstream pathways, which succeed in different functional cortical networks for sensorimotor control and multisensory integration, as well as hippocampal structures for allocentric representation of the environment. Based on multimodal imaging data, the current study provides a comprehensive framework for verticality processing in distinct brainstem to cortex streams passing through specialized thalamic nuclei, which is adaptive to various functional requirements. In this concept, *crossed* graviceptive pathways via the MLF/ATD and PPRF are connecting via the VPM/VPL and Pf/CM to the somatosensory and motor cortex to provide the signal input and reference frame for a robust execution of motor, postural, and locomotor commands relative to gravity.[50] This organization principle also allows for harmonization with ocular motor control, as vestibular inputs to midbrain centers for gaze control in roll and pitch are also conveyed mostly via the MLF. *Uncrossed* graviceptive pathways via the IVTT/ML in turn would bypass the ocular motor centers and reach the multisensory PIVC via the VPI. Functionally, this route is dedicated to the perception of verticality in concert with other sensory sources and the fast adaptation to variable external and internal stimuli.

Clinical Relevance of Verticality Processing for Higher Level Control of Body Posture

Decoding of the thalamocortical pathways and networks for verticality processing may be relevant for understanding the pathophysiology of various higher level (cortical) balance disorders. Thalamocortical graviceptive dysfunction, for example, contributes to body misalignment in pusher syndrome, in parkinsonian syndromes with postural instability and falls (such as advanced Parkinson disease or progressive supranuclear palsy), or in patients with chronic Vim DBS for tremor. Unilateral affection of thalamocortical networks of verticality perception leads to lateralized postural imbalance (in roll plane), whereas bilateral damage causes body misalignment in the anterior–posterior axis (in pitch plane).[1] Examples of the latter are found in various higher level balance disorders

such as vascular encephalopathy, normal pressure hydrocephalus, and neurodegenerative disorders. From a therapeutic perspective, networks of higher level verticality processing should be considered as a promising target for noninvasive transcranial neuromodulation or for connectome-based placement and volume of tissue activated-based optimal tuning of thalamic DBS.

Limitations

To allow for a sufficient number of cases for the analysis of ipsiversive versus contraversive tilts, all lesions were flipped to the right side. Our data showed similar structural and functional connectivity results for left versus right thalamic infarcts. Based on this, it is our interpretation that sensory processing in the thalamus is sufficiently similar to allow for the flipping of the lesions.

The use of a sample of healthy subjects for the connectivity analysis might present a potential confounder, as interindividual variability of structural and functional connections might not have been conclusively taken into account. This potential limitation is outweighed by the increase in data quality and the number of healthy subjects that can be analyzed. In addition, the microenvironment close to the ischemic lesion presents potential confounders for structural and functional connectivity analyses in the patient group.[51,52]

Conclusions

Our data based on multivariate SVR-LSM in a large cohort of patients with unilateral thalamic stroke clearly indicate the existence of distinct regions within the thalamus that are associated with side-specific verticality processing. The structural and functional connectivity analysis revealed a network architecture for verticality perception that connects the lower brainstem with different thalamic nuclei and the multisensory vestibular, somatosensory, and motor cortex for an optimal embedding of vestibular graviceptive signals in multisensory perception and motor control. These sensorimotor circuits allow fast modulation of head and body position in 3D space.

Author Contributions

J.C., B.B., A.Z., and M.D. contributed to the conception and design of the study, acquisition and analysis of the data, and drafting the manuscript and figures. L.E., R.M.R., and R.B. contributed to the acquisition and analysis of the data, and drafting the manuscript and figures.

Acknowledgments

Potential Conflicts of Interest

Nothing to report.

Data Availability Statement

The lesion maps from the Munich cohort will be publicly available upon publication (https://osf.io/4shmb/). The Mainz cohort is not publicly available due to lack of consent for data sharing by the patients.

References

1. Dieterich M, Brandt T. The bilateral central vestibular system: its pathways, functions, and disorders. Ann N Y Acad Sci 2015;1343: 10–26.

2. Mackrous I, Carriot J, Jamali M, Cullen KE. Cerebellar prediction of the dynamic sensory consequences of gravity. Curr Biol 2019;29: 2698–2710.

3. Cullen KE. The vestibular system: multimodal integration and encoding of self-motion for motor control. Trends Neurosci 2012;35: 185–196.

4. Angelaki DE, Cullen KE. Vestibular system: the many facets of a multimodal sense. Annu Rev Neurosci 2008;31:125–150.

5. Lang W, Büttner-Ennever JA, Büttner U. Vestibular projections to the monkey thalamus: an autoradiographic study. Brain Res 1979;177: 3–17.

6. Akbarian S, Grüsser OJ, Guldin WO. Thalamic connections of the vestibular cortical fields in the squirrel monkey (Saimiri sciureus). J Comp Neurol 1992;326:423–441.

7. Blum PS, Day MJ, Carpenter MB, Gilman S. Thalamic components of the ascending vestibular system. Exp Neurol 1979;64:587–603.

8. Blum PS, Gilman S. Vestibular, somatosensory, and auditory input to the thalamus of the cat. Exp Neurol 1979;65:343–354.

9. Elwischger K, Rommer P, Prayer D, et al. Thalamic astasia from isolated centromedian thalamic infarction. Neurology 2012;78:146–147.

10. Karnath HO, Johannsen L, Broetz D, Küker W. Posterior thalamic hemorrhage induces "pusher syndrome". Neurology 2005;64:1014–1019.

11. Roemmich R, Roper JA, Eisinger RS, et al. Gait worsening and the microlesion effect following deep brain stimulation for essential tremor. J Neurol Neurosurg Psychiatry 2019;90:913–919.

12. Baier B, Vogt T, Rohde F, et al. Deep brain stimulation of the nucleus ventralis intermedius: a thalamic site of graviceptive modulation. Brain Struct Funct 2017;222:645–650.

13. Dieterich M, Brandt T. Thalamic infarctions: differential effects on vestibular function in the roll plane (35 patients). Neurology 1993;43: 1732–1740.

14. Baier B, Conrad J, Stephan T, et al. Vestibular thalamus: two distinct graviceptive pathways. Neurology 2016;86:134–140.

15. Zwergal A, la Fougère C, Lorenzl S, et al. Functional disturbance of the locomotor network in progressive supranuclear palsy. Neurology 2013 Feb;80:634–641.

16. Dieterich M, Brandt T. Ocular torsion and tilt of subjective visual vertical are sensitive brainstem signs. Ann Neurol 1993;33:292–299.

17. Conrad J, Habs M, Ruehl RM, et al. White matter volume loss drives cortical reshaping after thalamic infarcts. Neuroimage Clin 2022;33: 102953.

18. Rorden C, Bonilha L, Fridriksson J, et al. Age-specific CT and MRI templates for spatial normalization. Neuroimage 2012;61:957–965.

19. Zhang Y, Kimberg DY, Coslett HB, et al. Multivariate lesion-symptom mapping using support vector regression. Hum Brain Mapp 2014;35: 5861–5876.

20. DeMarco AT, Turkeltaub PE. A multivariate lesion symptom mapping toolbox and examination of lesion-volume biases and correction methods in lesion-symptom mapping. Hum Brain Mapp 2018;39: 4169–4182.

21. Wiesen D, Karnath HO, Sperber C. Disconnection somewhere down the line: multivariate lesion-symptom mapping of the line bisection error. Cortex 2020;133:120–132.

22. Foulon C, Cerliani L, Kinkingnéhun S, et al. Advanced lesion symptom mapping analyses and implementation as BCBtoolkit. Gigascience 2018;7:1–17.

23. Conrad J, Boegle R, Ruehl RM, Dieterich M. Evaluating the rare cases of cortical vertigo using disconnectome mapping. Brain Struct Funct 2022;227:3063–3073.

24. Rojkova K, Volle E, Urbanski M, et al. Thiebaut de Schotten M. Atlasing the frontal lobe connections and their variability due to age and education: a spherical deconvolution tractography study. Brain Struct Funct 2016;221:1751–1766.

25. Catani M. *Thiebaut de Schotten M*. Atlas of Human Brain Connections: Oxford University Press, 2012.

26. Klein A, Andersson J, Ardekani BA, et al. Evaluation of 14 nonlinear deformation algorithms applied to human brain MRI registration. Neuroimage 2009;46:786–802.

27. Avants BB, Tustison NJ, Song G, et al. A reproducible evaluation of ANTs similarity metric performance in brain image registration. Neuroimage 2011;54:2033–2044.

28. Van Essen DC, Ugurbil K, Auerbach E, et al. The human connectome project: a data acquisition perspective. Neuroimage 2012;62:2222–2231.

29. Glasser MF, Sotiropoulos SN, Wilson JA, et al. The minimal preprocessing pipelines for the human connectome project. Neuroimage 2013;15:105–124.

30. Smith SM, Beckmann CF, Andersson J, et al. Resting-state fMRI in the human connectome project. Neuroimage 2013;15:144–168.

31. Whitfield-Gabrieli S, Nieto-Castanon A. Conn: a functional connectivity toolbox for correlated and anticorrelated brain networks. Brain Connect 2012;2:125–141.

32. Edlow BL, Mareyam A, Horn A, et al. 7 Tesla MRI of the ex vivo human brain at 100 micron resolution. Sci Data 2019;6:244.

33. Schmahmann JD. Vascular syndromes of the thalamus. Stroke 2003; 34:2264–2278.

34. Conrad J, Baier B, Dieterich M. The role of the thalamus in the human subcortical vestibular system. J Vestib Res 2014;24:375–385.

35. Deecke L, Schwarz DW, Fredrickson JM. Vestibular responses in the rhesus monkey ventroposterior thalamus. II. Vestibulo-proprioceptive convergence at thalamic neurons. Exp Brain Res 1977;30:219–232.

36. Liedgren SR, Milne AC, Schwarz DW, Tomlinson RD. Representation of vestibular afferents in somatosensory thalamic nuclei of the squirrel monkey (Saimiri sciureus). J Neurophysiol 1976;39:601–612.

37. Büttner U, Lang W. The vestibulocortical pathway: neurophysiological and anatomical studies in the monkey. Prog Brain Res 1979;50:581–588.

38. Akbarian S, Grüsser OJ, Guldin WO. Corticofugal connections between the cerebral cortex and brainstem vestibular nuclei in the macaque monkey. J Comp Neurol 1994;339:421–437.

39. Akbarian S, Grüsser OJ, Guldin WO. Corticofugal projections to the vestibular nuclei in squirrel monkeys: further evidence of multiple cortical vestibular fields. J Comp Neurol 1993;332:89–104.

40. Abraham L, Copack PB, Gilman S. Brain stem pathways for vestibular projections to cerebral cortex in the cat. Exp Neurol 1977;55:436–448.

41. Carpenter MB, Hanna GR. Lesions of the medial longitudinal fasciculus in the cat. Am J Anat 1962;110:307–331.

42. Zwergal A, Büttner-Ennever J, Brandt T, Strupp M. An ipsilateral vestibulothalamic tract adjacent to the medial lemniscus in humans. Brain 2008;131:2928–2935.

43. Baier B, Thomke F, Wilting J, et al. A pathway in the brainstem for roll-tilt of the subjective visual vertical: evidence from a lesion-behavior mapping study. J Neurosci 2012;32:14854–14858.

44. Zwergal A, Strupp M, Brandt T, Büttner-Ennever JA. Parallel ascending vestibular pathways: anatomical localization and functional specialization. Ann N Y Acad Sci 2009;1164:51–59.

45. Yang TH, Oh SY, Kwak K, et al. Topology of brainstem lesions associated with subjective visual vertical tilt. Neurology 2014;82:1968–1975.

46. Baier B, Bense S, Dieterich M. Are signs of ocular tilt reaction in patients with cerebellar lesions mediated by the dentate nucleus? Brain 2008;131:1445–1454.

47. Jones EG. The Thalamus. Cambridge University Press, Cambridge, United Kingdom, 2007.

48. Kirsch V, Keeser D, Hergenroeder T, et al. Structural and functional connectivity mapping of the vestibular circuitry from human brainstem to cortex. Brain Struct Funct 2016;221:1291–1308.

49. Karolis VR, Corbetta M, Thiebaut de Schotten M. The architecture of functional lateralisation and its relationship to callosal connectivity in the human brain. Nat Commun 2019;10:1417.

50. Ilyas A, Pizarro D, Romeo AK, et al. The centromedian nucleus: anatomy, physiology, and clinical implications. J Clin Neurosci 2019;63:1–7.

51. Siegel JS, Snyder AZ, Ramsey L, et al. The effects of hemodynamic lag on functional connectivity and behavior after stroke. J Cereb Blood Flow Metab 2016;36:2162–2176.

52. Jellison BJ, Field AS, Medow J, et al. Diffusion tensor imaging of cerebral white matter: a pictorial review of physics, fiber tract anatomy, and tumor imaging patterns. Am J Neuroradiol 2004;25:356–369.

53. Ilinsky I, Horn A, Paul-Gilloteaux P, et al. Human motor thalamus reconstructed in 3D from continuous sagittal sections with identified subcortical afferent territories. eNeuro 2018;5:1–17.